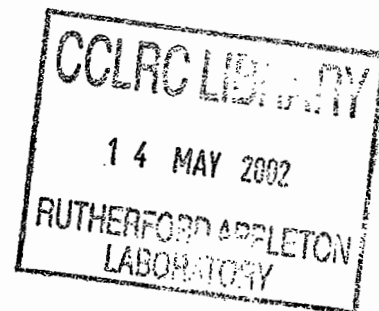**CLRC**

Electron-volt spectroscopy at a pulsed neutron source using a resonance detector technique

C Andreani A Pietropaulo R Senesi G Gorini M Tardocchi
A Bracco N Rhodes and E Schooneveld

30th April 2002

COUNCIL FOR THE CENTRAL LABORATORY OF THE RESEARCH COUNCILS

Electron-volt spectroscopy at a pulsed neutron source using a resonance detector technique

C. Andreani, A. Pietropaolo, R. Senesi

Dipartimento di Fisica, Università degli Studi di Roma Tor Vergata
and INFM UdR Tor Vergata, via della Ricerca Scientifica 1, 00133 Roma, Italy.

G. Gorini, M. Tardocchi

Dipartimento di Fisica "G.Occhialini", Università degli Studi di Milano-Bicocca,
and INFM, UdR Milano-Bicocca, Milano, Italy

A. Bracco

Dipartimento di Fisica, Università degli Studi di Milano
and INFN, Sezione di Milano, Milano, Italy

N. Rhodes, E.Schooneveld

Rutherford Appleton Laboratory, ISIS Facility, Chilton, Didcot, OX11 0QX, UK

Abstract

The effectiveness of the neutron resonance detector spectrometer for Deep Inelastic Neutron Scattering measurements has been assessed by measuring the Pb scattering on the eVS spectrometer at ISIS pulsed neutron source and natural U foils as (n,γ) resonance converters. A conventional NaI scintillator with massive shielding has been used as γ detector. A neutron energy window up to 90 eV, including four distinct resonance peaks, has been assessed. A net decrease of the intrinsic width of the 6.6 eV resonance peak has also been demonstrated employing the double difference spectrum technique, with two uranium foils of different thickness.

INTRODUCTION

In the last years the high flux of neutrons well above 1 eV, available at the ISIS spallation neutron source, has opened this energy range to new spectroscopic studies in condensed matter. Inelastic scattering measurements with epithermal neutrons are now routinely performed with the eVS spectrometer at the ISIS facility [1-5]. This instrument represents a unique neutron spectrometer, in that it uses the high intensity of neutrons in the eV energy range and the pulsed nature of the ISIS source, to determine atomic momentum distributions and mean kinetic energies in a variety of systems. When the momentum transfer in the scattering process is sufficiently large (at least 10 times higher than the mean atomic momentum), the scattering can be interpreted within the "Impulse Approximation" (IA) [6], using the scattering technique known as Deep Inelastic Neutron Scattering (DINS) [7]. By measuring the energy and momentum change of the neutron, one can determine the momentum component of the target atom along the direction of the scattering vector $\mathbf{q}$. In the last years DINS has provided unique information in a variety of systems. These include hydrogen bonds [8], metal hydrides [9,10], catalysts [11], glasses [12,13], amorphous materials [14], quantum fluids and solids [15-19]. Energy transfers in the 1-30 eV region and wavevector transfers in the range 30-200 Å^{-1} are currently accessed on eVS using a Single Difference Technique (SDT) [2]. The energy of the scattered neutron is fixed by a nuclear resonance absorption foil, i.e. ^{197}Au or ^{238}U foils, which strongly absorb neutrons over narrow energy ranges, and the incident energy and hence energy and momentum transfers are determined using standard time of flight techniques. The absorption foil is cycled in and out of thescattered neutron beam and two measurements are taken, one with the foil between sample and detector and one with the foil removed. The difference between these two data sets (i.e. the number of neutrons absorbed by the foil) is the experimental signal and provides a measurement of the intensity of neutrons scattered with final energy E_1, determined by the resonance of the foil. The SDT is used on eVS for high-q scattering measurements with ^{6}Li-glass scintillators currently employed as neutron detectors [20]. However, so far this kind of scattering measurements is limited to a final energy range 1-20 eV [6], for at higher neutron energies scintillator detectors become rather inefficient and suffer from excessive background rates with ensuing dead-time problems.

There is a considerable interest in extending measurements with the DINS technique into the 10-100 eV region [21-24]. Indeed this possibility would allow to address new experimental studies in condensed matter systems, such as the dispersion relations of high energy excitations in metals (e.g. Stoner excitations, excitons, polarons, etc. in semiconductors and insulators), high lying molecular rational-vibrational states, molecular electronic excitations, electronic level in solids, which at the moment can only be investigated by electromagnetic probes and often not in bulk materials. For this reason, in the recent past, alternative approaches for neutron spectroscopy

at eV neutron energies have been proposed. In particular an interesting method, which would allow the extension, in both higher q and $\hbar\omega/2\pi$, of the kinematical range accessible on eVS, appears to be the Resonance Detector Technique (RDT) [25-29]. In this technique the (n,γ) reaction is used and the energy of the scattered neutrons assigned by measuring the prompt γ cascade from the absorbing foil with a γ detector. As in SDT the final neutron energy is still defined by the resonance itself, whereas the incoming neutron energy is determined by the neutron time of flight. A clear advantage of RDT is that the signal is the direct measurement, rather than a difference between two large count rates, i.e. foil in and foil out, so that statistical accuracy is better. However in this case special attention has to be devoted to keep the background rate to a very low level.

In this paper we report experimental results of DINS measurements performed on eVS on polycrystalline Pb and ^{4}He/H$_2$ fluid mixture samples using the RDT method. Aim of these measurements was to test the potential of the RDT approach on the eVS spectrometer for DINS in the energy range 10-100 eV. A conventional NaI scintillator was used for γ detection because of its good light yield. Previous attempts at using this kind of detector [28] were quickly abandoned due to its high γ background sensitivity [30]. In our experiments a massive γ/n shield was therefore used to bring down the background rate to a manageable level. Simultaneous measurements were also performed with a standard ^{6}Li-glass scintillator using the SDT method, in order to evaluate the performance and effectiveness of the NaI scintillator in comparison with these scintillator detectors currently used on eVS. Two resonance foils, i.e. U and Ta, have been chosen to define the final scattered neutron energy. For the Pb measurement with the RDT method, spectra from U foils of two different thicknesses have also been recorded. The latter choice aimed to test the Double Difference Technique (DDT) [31]. In this case the scattered signal is obtained by the weighted difference of signals coming from U foils of distinct thickness. This method achieves a finer experimental resolution than the SDT one, by removing the Lorentzian wings coming from the resonance foil. It has to be stressed that in the RDT approach the DDT requires only a single difference spectrum between signals coming from two foils of different thickness. On the other hand in the SDT approach a foil-out measurement must in any case be performed in addition to the two diffent thickness foil-in measurements.

2   EXPERIMENT

The experiment was carried out at ISIS at the Rutherford Appleton Laboratory (UK) [2], on the Electron Volt Spectrometer (eVS). The energy spectrum of the neutrons incident on the scattering sample is typical of an undermoderated spallation neutron source, i.e. it peaks at ≈0.03 eV and falls
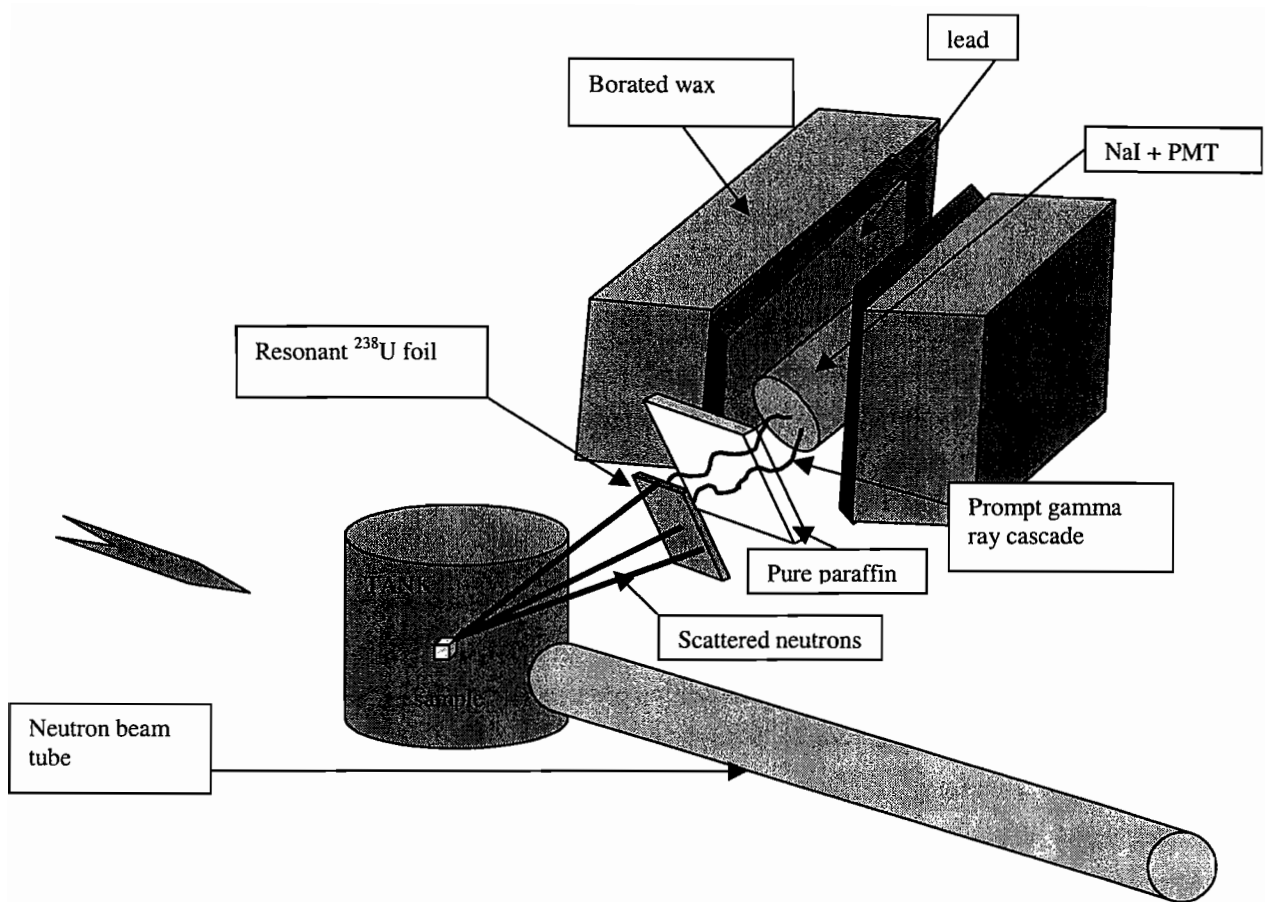
Figure 1. *Experimental set up for the deep inelastic scattering experiment on eVs with the NaI and* *⁶Li-glass detectors.*

off as $\approx 1/E$ in the epithermal region. In the experiments reported here the neutrons were scattered by a polycrystalline Pb and ^{4}He/H$_2$ fluid mixture samples with an experimental set-up of illustrated in Fig. 1. The Li-glass scintillators and the NaI detector were both placed in forward geometry (see Table I). The NaI detector, 8 cm diameter by 8 cm length, was collecting the prompt γ's, emitted isotropically, following the neutron capture reaction in the resonance foil. The NaI detector was oriented with the axis orthogonal to the incoming neutron beam direction. The resonance foil was placed as close as possible to the NaI surface and oriented with its axis at an angle of 18° to the scattered neutron direction. In this arrangement the effective foil thickness was 5% higher than the nominal thickness, t (see Table I), and the apparent foil area was about 5% lower than the nominal foil area (see Table I). With the described set-up the detection solid angle for the NaI detector resulted in 0.29 sterad, 3% of the γ's were therefore intercepted by the detector.

The scattering geometry was chosen in order to achieve both sufficient detection efficiency and adequate shielding of the NaI detector. The shielding consisted of lead blocks (5-cm thick) placed around the detector assembly and borated wax (15-cm thick) on the outside. We observed that a 5-cm thick lead layer effectively shielded the NaI from γ rays produced, after neutron capture, by the surrounding concrete, steel and ^{10}B in the eVS blockhouse. An important background contribution is due to epithermal neutron absorption in elements such as Sb, U, I, Ta, and B present in the shielding and the detecting apparatus.

Further measures to suppress background events (in addition to the use of a massive shielding) were i) the rejection of events below a preset energy threshold (below 0.8 MeV) and ii) the use of a paraffin slab shield (15x15x5 cm^3) between the foil and the NaI detector. Due to the limited beam-time available, these background suppression measures were not tested separately. Their overall effectiveness is demonstrated in Fig. 2 where background spectra for different conditions are compared. The paraffin front shield is effective in attenuating the direct epithermal neutron flux on the detector and lead shield, allowing for the suppression of resonant neutron absorption peaks coming from iodine and impurities present in the Pb shield and the NaI scintillator.
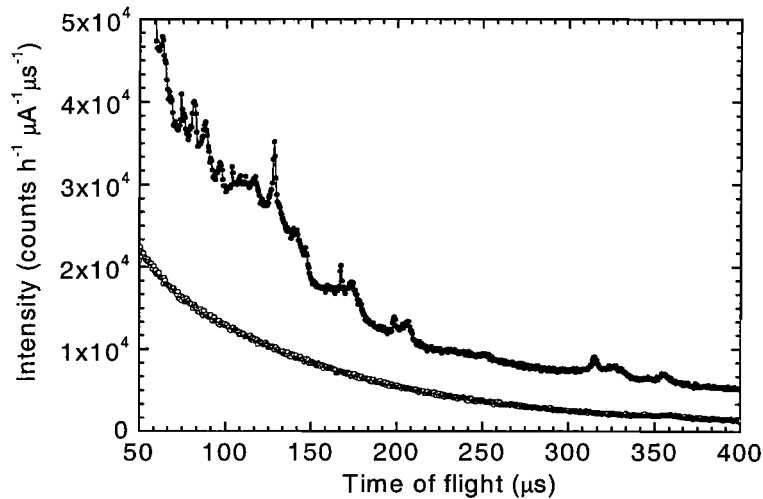

Figure 2. *Background spectra for a Pb sample recorded with a NaI scintillator under different shielding and discrimination conditions. The open circles are for the case where a front paraffin shielding and a 0.8 MeV discrimination threshold have been used. No front shield and no discrimination are used in the full circles case.*

It is interesting to compare the background sensitivity of our NaI scintillator and the one of the conventional ^{6}Li-glass scintillator. In Fig. 3 the time of flight spectra from a Pb sample are

shown for NaI and ^{6}Li-glass measurements using the same 30 μm thick Uranium foil. The peaks correspond to the 6.67 eV ^{238}U resonance. The peak intensity is lower in the NaI case, indicating a lower overall efficiency due to the non-optimal detector set-up. More interesting is the signal/background ratio, which is similar in the two spectra. It has to be stressed that the continuos line in Fig. 3(a) is a guide for the eye describing the γ background level shown in Fig. 2 (open circle), while the continuos line in Fig. 3(b) shows the foil out scattering spectrum.

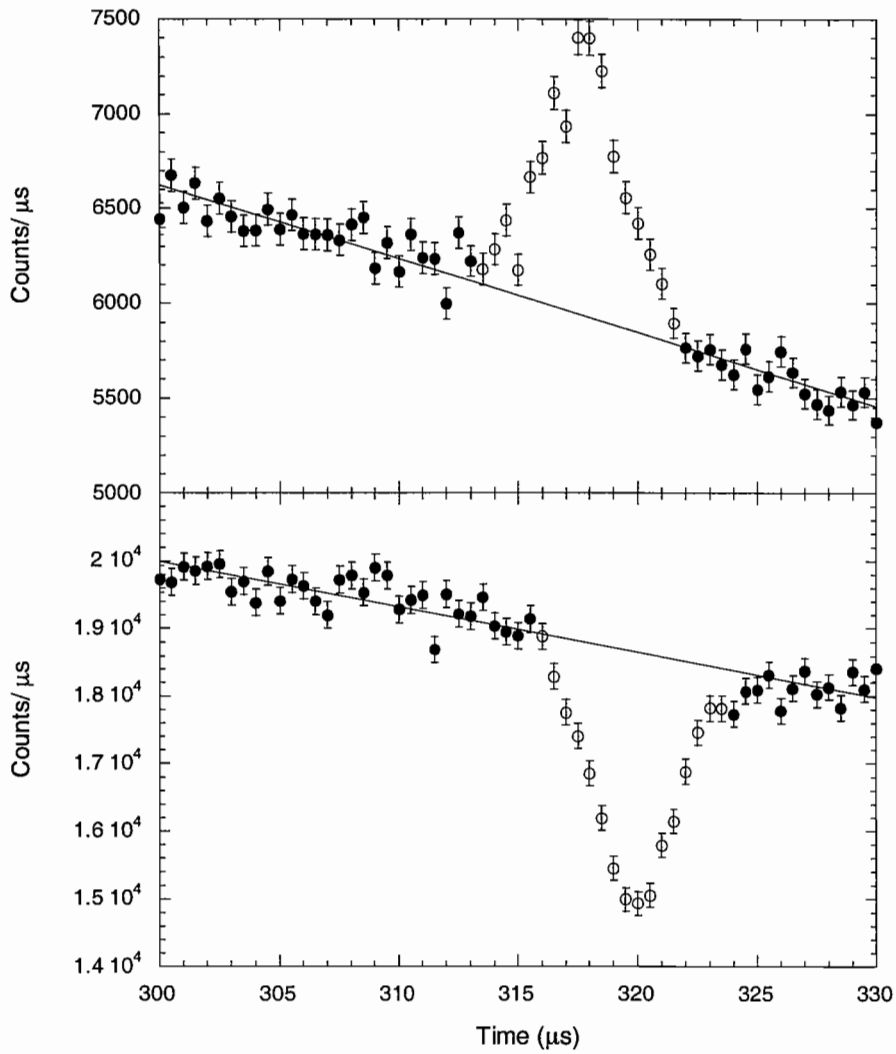**Figure 3**. *Neutron time of flight spectra from a lead sample recorded using a 30 μm thick uranium foil in the experimental set-up of Fig.1. The NaI spectrum (top) has a peak corresponding to the 6.67 eV ^{238}U resonance. The same resonance gives rise to the absorption peak in the ^{6}Li-glass spectrum (bottom).*

The data collection system was based on a standard NIM interface. Two independent electronics chains were used for simultaneous measurements of energy and time of flight (TOF) spectra. The output from the anode of the PM-tube was split and sent to two separate timing filter amplifiers. A timing filter amplifier was used in the energy channel chain instead of a standard spectroscopy amplifier fed with the preamplifier output from the PM-tube. Most TOF spectra were collected with a discrimination threshold set to accept all events above 800 keV, while no discrimination was applied to pulse height spectra. As expected, due to the poor energy resolution of the NaI detector ($\Delta E/E$=6.8% at E_γ=1 MeV) and high sensitivity to background, the pulse height spectrum did not allow any strong feature to be revealed. The γ-energy discrimination in the TOF chain was therefore not feasible. The TOF channel consisted of a timing filter amplifier plus discriminator. The output of the discriminator was sent to the standard ISIS data acquisition electronics (DAE) for recording the TOF spectra.

The material chosen as resonance foil in the present experiment was ^{238}U (see Table I). Two different ^{238}U foils, i.e. 30 and 120 μm thick, were used in order to employ the DDT method with the NaI detector and check the improvement in experimental energy resolution expected [31]. Indeed this method consists of deriving the scattering signal as a linear combination of measurements of two thicknesses of the same foil material. The resulting energy resolution is then expected to be better than either foil alone, i.e. using the SDT, although at the expenses of signal intensity.

Table I. *Summary of DINS measurements performed on the Lead sample, using NaI and ^{6}Li detectors. IC represents the Integrated Proton Current, 2θ represents the scattering angle and W_G and W_G, the HWHM of Gaussian and Lorentzian components obtained from the fitting procedure (see text).*

Technique	Filter	Detector	IC (μAh)	2θ (degrees)	W_L(A^{-1})	W_G (A^{-1})
RDT	^{238}U, t=30μm	NaI	900	38±10	85±5	182±18
SDT	^{238}U, t=30μm	^{6}Li	900	37±2	85±5	173±7
RDT	^{238}U, t=30μm	NaI	900	38±10	64±5	182±18
RDT	^{238}U, t=120μm	NaI	190	38±10		

The summary of the measurements with a polycrystalline Pb sample (10x10 cm^2 and 1 mm thick) performed on the eVS spectrometer are reported in Table I. Measured time of flight spectra were normalized with respect to the incident monitor intensity and the integrated proton current. Subsequently they were corrected for the γ background. The latter is sample dependent and was
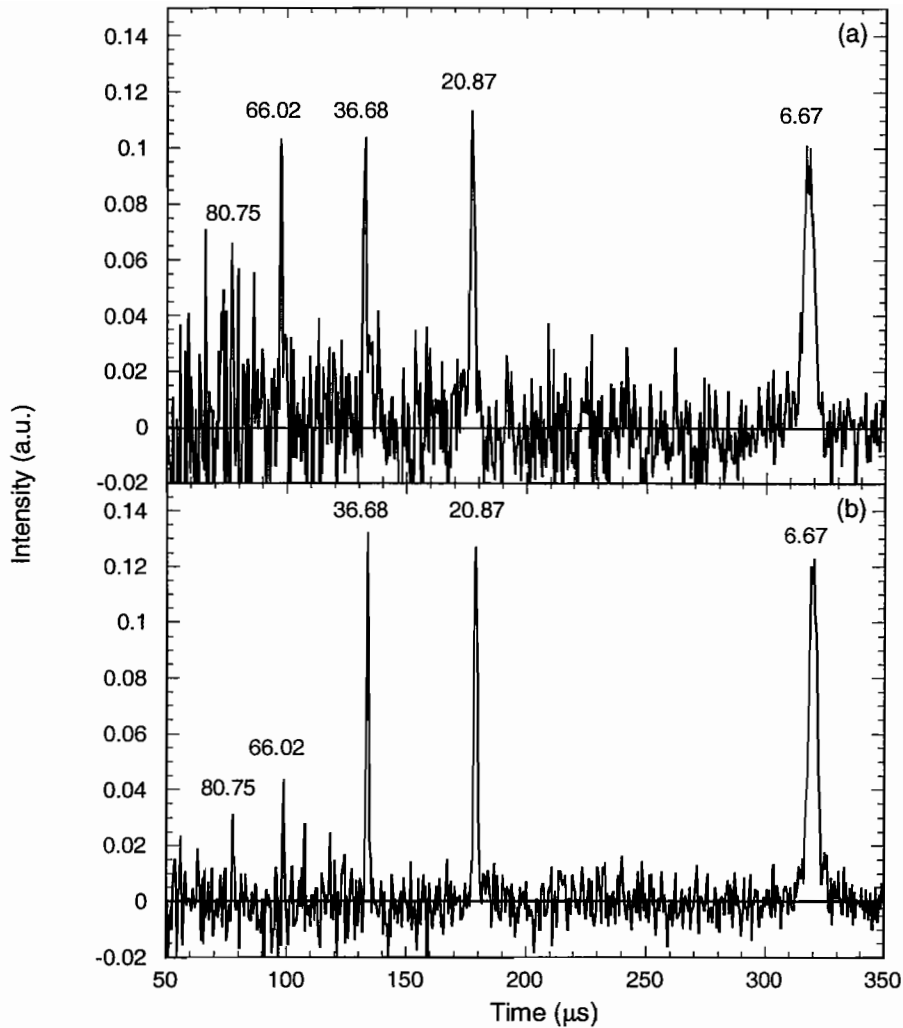
Figure 4. (a) *Measured time of flight spectra from Pb recorded by the NaI detector for the case of a 30μm ^{238}U foil, corrected for background. The spectrum is normalized so that the area under the 6.67 eV peak amounts to one count. Additional peaks are marked by the associated energy of the ^{238}U resonances.*

(b) *same as (a) but recorded by the ^6Li glass scintillator. Normalization is the same as for case (a).*

measured with the Pb slab in the sample position without the resonant uranium filter. An example of the resulting (background subtracted) time of flight spectra from Pb are shown in Fig. 4 for the case of a 30 μm ^{238}U foil, from both the NaI scintillator and the ^6Li scintillator. Both spectra are normalized so that the area under the 6.67 eV peak amounts to one count. In Fig. 4(a) additional peaks are clearly visible, corresponding to scattering signals from lead at final neutron energies

defined by the ^{238}U resonances, i.e. 20.9 eV, 36.7 eV, and 66.0 eV [32]. Above 80 eV the statistical noise is too large and the identification of additional peaks is not possible. The area under the peaks decreases with increasing resonant energy; it is only 0.20 at 66.0 eV. In Fig. 4(b) the time of flight spectrum recorded by the Li-glass scintillator shows a stronger decrease of peak intensities with increasing resonant energy: the area under the 66.0 eV peak is only .08, i.e. about 2.5 times lower, in relative terms, than the corresponding peak in the NaI spectrum. This is mainly due to the inverse velocity dependence of ^{6}Li neutron absorption cross section. The stronger peak intensity at high neutron energies is a principle advantage of the RDT over the SDT for detection of high-energy neutrons.

3 DATA ANALYSIS

The time of flight scattering intensities plotted in Fig. 4 represent the number of counts collected in a time channel of width Δt centred in t, expressed by [2]:

$$C(t)\Delta t = I(E_0)\frac{dE_0}{dt}\Delta t N \frac{d^2\sigma}{d\Omega dE_1}\eta(E_1)\Delta\Omega\Delta E_1 \qquad (1)$$

where $I(E_0)\dfrac{dE_0}{dt}\Delta t$ is the number of incident neutrons per square centimetre, N is the number of scattering atoms, $\Delta\Omega$ is the detector solid angle, ΔE_1 the energy resolution of the analyser, $\eta(E_1)$ is the detector efficiency, and $\dfrac{d^2\sigma}{d\Omega dE_1}$ is the partial differential scattering cross section. The latter quantity is related to the dynamic structure factor $S(q,\omega)$ via:

$$\frac{d^2\sigma}{d\Omega dE_1} = b^2 \frac{k_0}{k_1} S(q,\omega) \qquad (2)$$

where b is the scattering length, k_0 and k_1 are the initial and final state neutron wave vectors. The applicability of IA relies on two assumptions. The first is that the momentum transfer, q, is sufficiently large for the scattering to be incoherent and the second is that the struck atom gains sufficient energy from the neutron for its `recoil' to be that of a free atom. It has been shown in previous work that the IA is reached as the momentum transfer q goes to infinity [33]. Due to the large values of the momentum and energy transfers accessed in the present measurements the experimental data have been analysed within the IA framework. When in the IA regime, the dynamic structure factor is related to the single particle momentum distribution, $n(p)$, by [6]:

8

$$S_{IA}(q,\omega) = \int n(p)\delta\left(\omega - \omega_R - \frac{p \cdot q}{M}\right)dp \qquad (3)$$

where $\omega_R = q^2/2M$ is the recoil energy of the struck atom of mass M and the argument of the δ-function expresses the conservation of energy and momentum. The momentum distribution is usually expressed in terms of the West scaling variable, y which represents the component of q along the scattering direction and is defined by [34]:

$$y = \frac{M}{q}(\omega - \omega_R) \qquad (4)$$

One can then introduce a longitudinal momentum distribution or Compton Profile, $J(y)$, in terms of $S_{IA}(q,\omega)$:

$$J(y) = \frac{q}{M} S_{IA}(q,\omega) \qquad (5)$$

where $J(y)$ is the probability that an atom has a momentum distribution parallel to q of magnitude between y and $y+dy$. For an isotropic system $J(y)$ is the probability that an atom has a component of momentum between y and $y+dy$ in any arbitrary direction. Physically, y scaling in IA implies that the Compton profile should be symmetric and have its maximum at $y=0$. Therefore, deviations in the symmetry and position of the profile peak provide valuable information on the validity of the IA [33]. The single particle mean kinetic energy, $<E_K>$, is related to the second moment of $J(y)$ via:

$$\int_{-\infty}^{+\infty} y^2 J(y)dy = \sigma_y^2 = \frac{2M}{3}\langle E_K \rangle \qquad (6)$$

where σ_y is the standard deviation of the Compton profile.

The experimental Compton profile for the n-th detector is expressed by:

$$F_n(y) = J(y) \otimes R_n(y) \qquad (7)$$

where $R_n(y)$ is the experimental energy resolution. The resolution function of a resonance inverse instrument like eVS, described in detail in previous papers [35], has two main components, one coming from the uncertainties in the neutron path from moderator to detector (geometrical component), the other generated by the uncertainty associated to the energy value at which neutrons are absorbed by the foil after scattering by the sample (energy component). The former, resulting from several distinct distributions [35], is assumed to be Gaussian, the latter, is represented by a Voigt function, i.e. a convolution of a Lorentzian lineshape, coming from the

Breit-Wigner law for the nuclear resonances, with a Gaussian function which takes into account the Doppler broadening coming from the lattice motion. The Lorentzian component, due to the intrinsic shape of the nuclear resonance of the foil, is well known to be the unfortunate characteristic that mainly limits the experimental resolution function. Indeed its extensive wings, in a single peak difference count, and the infinite second moment prevent any significant reduction of the energy component of the resolution function. It was first suggested by Seeger et al. [31], that the Double Difference Technique (DDT) offers a method to overcome this problem. This method consists of performing an additional measurement using a thicker foil of the same resonance material and performing an appropriate linear combination of foil-out, thin foil-in and thick foil-in measurements. One chooses two analysing foils of the same material: a thin foil with a nuclear thickness $Nd=\alpha$ (N being the nuclear density of the absorber and d the analyser thickness) and a thick foil with $Nd=\alpha/\beta$, where $\beta<1$ [31]. Since the functional form of the wings scales linearly with thickness, in this way it is possible to eliminate much of the wing problem, inherent in the single difference method, by an appropiate weighted difference of thick and thin foil spectra. In the single difference method the attenuation profile across the resonance is given by $A(E)= 1-\exp(\sigma(E)Nd)$, where $\sigma(E)$ is the reaction cross section in the vicinity of a well separated resonance peak occurring in the eV region, described by the Breit-Wigner expression [36]:

$$\sigma(E) = \frac{\sigma_0}{1+4(E-E_R)/\Gamma^2} \tag{8}$$

where σ_0 is the cross section at $E=E_R$ and Γ is the total resonance width. Normalising to the foil out counts I_{out}, the double difference counts at the resonance energy are given by [31]:

$$I_{peak}^{DDT} = I_{out}\left(1-\beta-e^{\sigma_0\alpha}+\beta e^{\sigma_0\alpha/\beta}\right) \tag{9}$$

The double difference function provides a finite second moment and a much narrower HWHM [31].

4   RESULTS AND DISCUSSION

4.1   Lead sample

In the case of polycrystalline Pb at room temperature, the $J(y)$ function at the single scattering angle (see Table I) can be well described, within the harmonic approximation, by an isotropic Debye solid. For this reason this sample is routinely used as a standard reference material

for calibrating the instrumental resolution on eVS spectrometer [2]. The resulting Compton profile is a Gaussian lineshape with a standard deviation $\sigma_y=35.3\text{Å}^{-1}$ In Fig. 5 and Fig. 6 the experimental $F(y)$ functions (see eq. 7) for polycrystalline Pb are plotted. In Fig. 5 the Compton profiles were obtained from the time of flight spectrum, recorded by the NaI detector, selecting a 6.67 eV final energy with the 30 μm thick uranium foil, using the SDT. In this case the standard foil-in foil-out difference was used to obtain the experimental Compton profile. The $F(y)$ function was also obtained for the spectrum recorded with the thick U foil, using the DDT. In the latter a weighted difference of thick and thin foil was performed according to eq. (9). The $F(y)$ functions were fitted (see continuous line in 6(b) and dashed line in Fig. 6(b)) by a profile given by the convolution of the function $J(y)$ with the Voigt instrument resolution profile, $R(y)$, using a normalization factor as a free parameter. The fitting procedure, yielded a set of Half Width at Half Maximun (HWHM) values for both Gaussian, W_G and Lorentzian, W_L, components of the fitting function, which are listed in Table I for the ^{238}U foils at 30 μm and 120 μm thickness. The HWHM value for the Gaussian comes from three distinct contributions: the Doppler broadening of the resonance filter, the geometrical resolution component [35] and the Pb momentum distribution. The latter is also shown in Fig. 6(b). We stress that the Voigt instrument resolution, $R(y)$ obtained from both RDT and SDT approach, give the same profiles within the experimental uncertainties (see Table I).
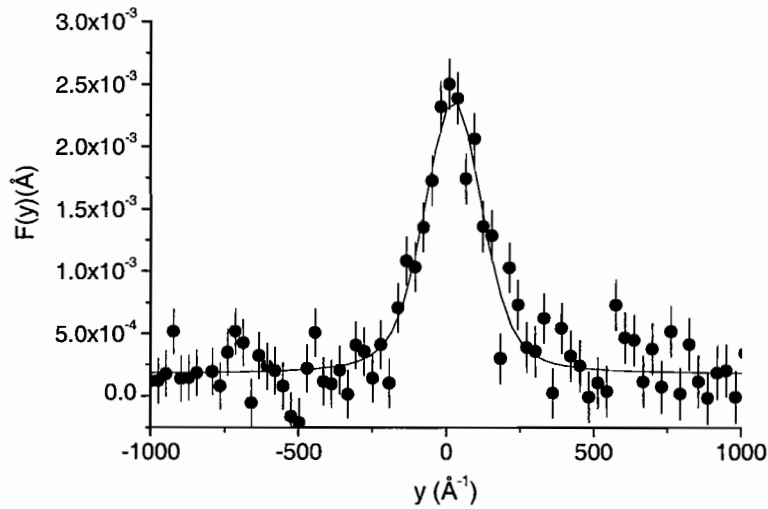

Figure 5. *Experimental response function F(y) from the NaI scintillator for the 30μm uranium foil at a final neutron energy of 6.67 eV. The error bars are statistical errors. Continuos line is the fit with a Voigtian function (see text).*

In principle the same analysis can be performed for the whole set of final energies of the U foil for both single and double difference method. However in the present experiment this analysis

was not possible as a consequence of the poor time binning which, due to the limited acquisition time and memory of the data acquisition electronics, was optimized for the low energy resonance only. Indeed we stress that the total Integrated Proton Current, (IC), reported in Table I, corresponds on average to one third of the typical IC used for DINS measurements on eVS.
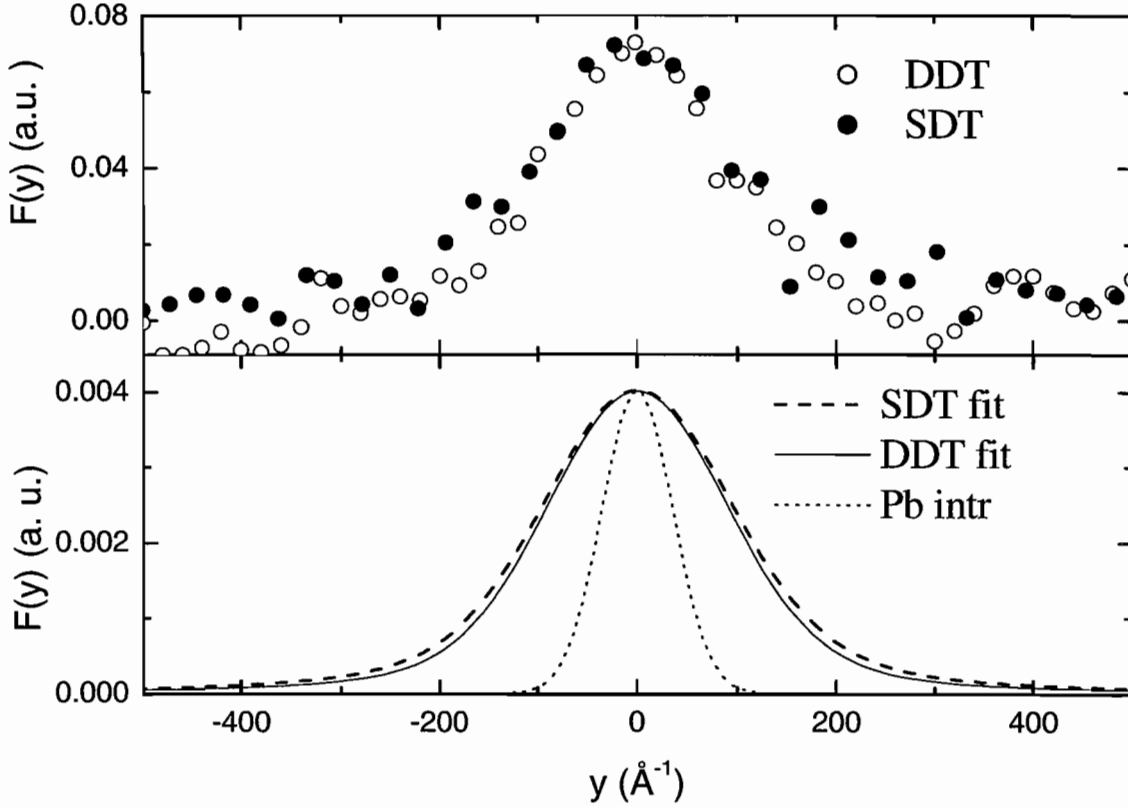

Figure 6. (a) *Experimental response function F(y)from the NaI γdetector for the 30μm uranium foil at a final neutron energy of 6.67 eV obtained from SDT (full dots) and DDT (open dots).*

(b) *Dashed line is the fit to the SDT spectrum, continuos line is the fit to the DDT spectrum (see text), dotted line is the Compton profileJ(y), from the Pb sample .*

While a quantitative analysis of deep inelastic scattering is best performed as described above, it is also possible to visualize the improved instrumental resolution resulting from the DDT by a direct analysis of the time of flight spectra shown in Fig. 7. In figure 7(a), the time of flight spectra in the 6.67 eV peak region are plotted for the three cases of thin foil, thick foil and DDT spectrum. In figure 7(b), three Gaussian curves fitting the spectra in (a) are shown. We note that the
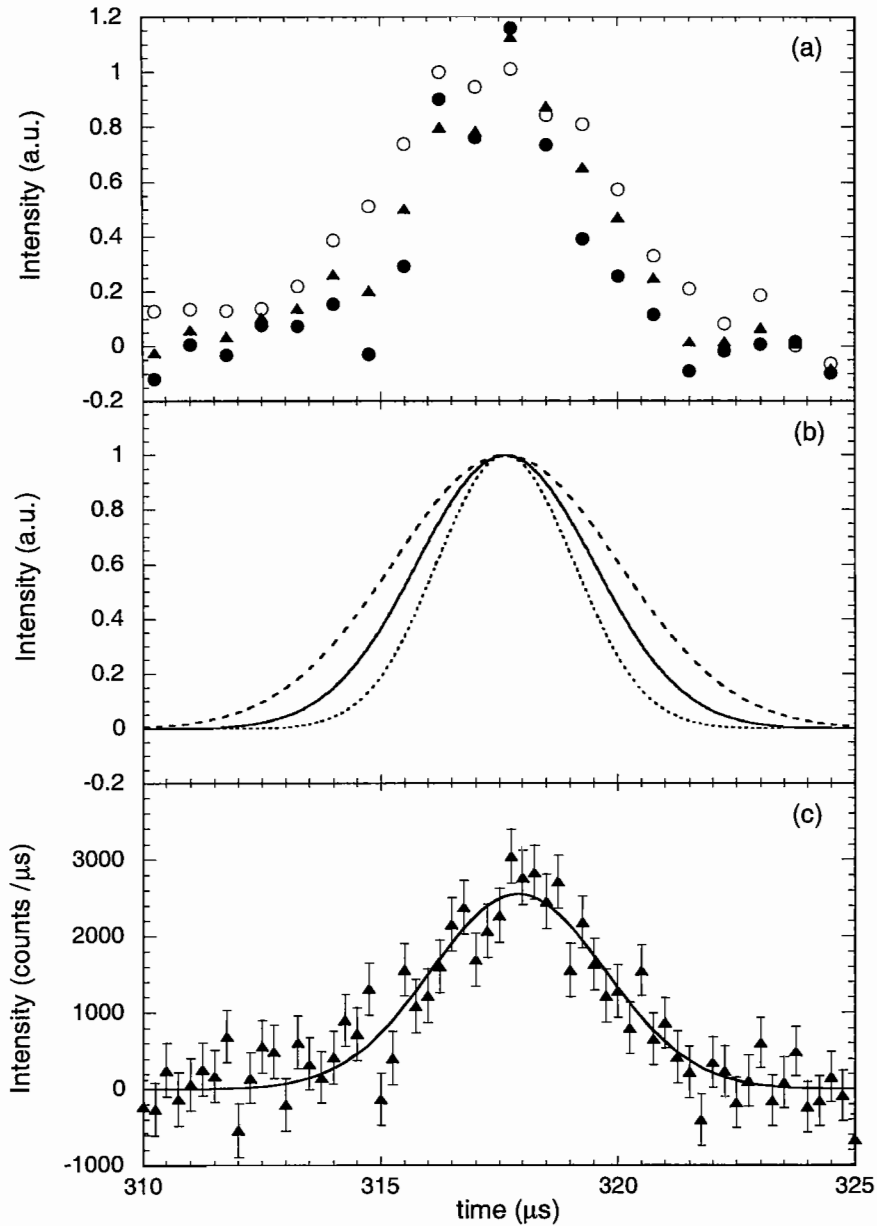
Figure 7. (a) *Time of flight spectra in the 6.67 eV peak region for the three cases of thin foil (triangle), thick foil (open circle) and DDT spectrum (solid circle) using lead sample, uranium foil and NaI detector. The spectra are normalised so that their Gaussian fits have unit intensity (height). The bin width is 1.5 μs.*

(b) *Gaussian curves fitting the spectra in (a), i.e. thin foil (continuous line), thick foil (dashed line) and DDT (dotted line).*

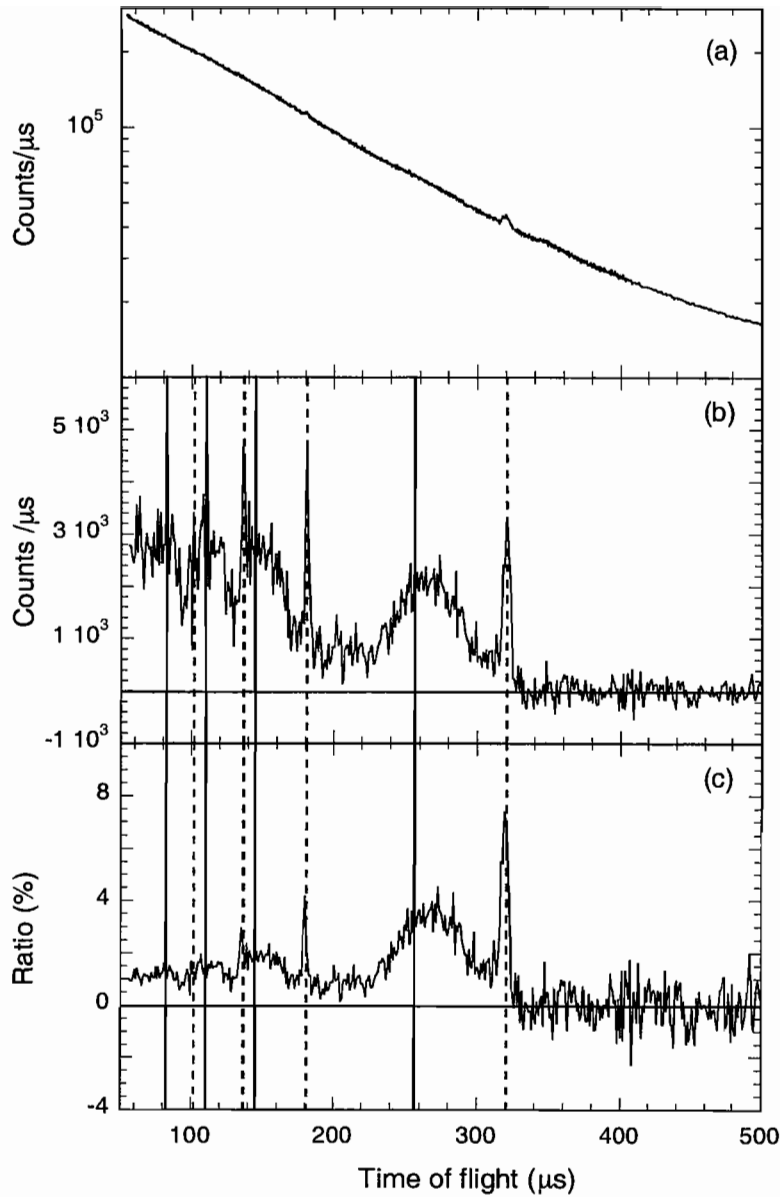(c) *Thin foil spectrum in (a) fitted with a Gaussian lineshape (continuous line from (b)). The bin width is 0.5 μs.*

13

Figure 8. *Neutron TOF spectra from a 50% ^{4}He-H_2 mixture measured with 120 μm thick ^{238}U foil and a NaI γ detector (Fig. 6a). The signal peaks can be identified on top of a large background component. The bin width is 0.25μs for t<400 μs . In (b) same spectrum as in (a) but after background subtraction (difference spectrum). The vertical lines mark the expected TOF values for neutron scattering on Al (dashed) and H (full) atoms assuming neutron final energies of 6.67, 20.9, 36.7 and 66.0 eV. A bin width of 1 μs is used to reduce statistical noise. In (c) ratio between the difference spectrum (b) and the foil-in spectrum (a) is plotted. A bin width of 1 μs is used to reduce statistical noise.*

width of the peak is narrowest for the DDT case demonstrating the improved resolution. In Fig. 7(c) we also show the Gaussian fit to the data for the thin foil case using a time resolution of 0.5 μs.

4.4 ^{4}He-H$_2$ samples

Neutron TOF spectra from ^{4}He-H$_2$ mixtures were recorded using both a thin and thick ^{238}U foil, as a test of the performance of the present RDT apparatus for samples of low atomic mass. An independent measurement of the background signal, with foil out, was also performed. In Fig. 8(a) and 8(b) the foil in signal and the background-corrected spectra are shown. From Fig.8(b) we observe that the relevant scattering from hydrogen and sample container (aluminum) occur in the time of flight region $t<$ 325 μs. In Fig. 8(c) the ratio between the difference (Fig. 8(b)) and signal (Fig.8(a)) spectra is also shown. Several observations can be made. The narrow peaks in the difference spectrum due to neutrons scattered from the Al sample holder, coming from four distinct values of the final energies, defined from the ^{238}U resonances are marked in the figure (dashed lines). The signals from hydrogen, coming from the 6.6 eV resonance energy, appear to be shifted to longer times with respect to their nominal position expected by the IA (full lines). This is an indication of the presence of Final State Effect (FSE) occuring at this low scattering angle from H mass [33]. The other H peaks coming from the higher U resonances are very poorly defined and, due to the poor statistics and smaller scattering cross section, the helium recoiling peak, expected at an intermediate time of flight, is not observed. As a general comment from Fig. 8(c) we note that as far the signal/background ratio is concerned, the scattering signal events represent a small fraction of the total: the signal/total ratio, which should approach unity under low background conditions, is ≈4% for the 6.67 eV resonance, and decreases to values below 2% for the high energy resonances. For these reasons the analysis in y space performed for lead was not attempted for this sample.

5   CONCLUSIONS

The results obtained in this paper should be regarded as a first step towards the routinely use of the Resonant Detector Technique for spectroscopy of epithermal neutrons in the 1-100 eV range. A first result we stress is the successful use of a NaI detector for this application. Previous experiments [28] had discarded NaI in favour of BGO scintillators mainly because of their lower background. Yet the present results indicate that the use of NaI scintillators, in combination with a U converter foil, using the Resonant Detector approach, allows neutron spectroscopy measurements

in the energy range 1-10 eV. This finding is supported from Fig. 3 where we note that the achieved signal/background ratio for the NaI detector is comparable with that obtained from a standard ^{6}Li scintillator. Moreover in the latter case (see Fig. 3(b)) we stress that the foil out measurement represents an effective background level which is inherent in the SDT approach and for this reason cannot be avoided in the experimental technique. On the other hand the intrinsic advantage of the RDT approach, is that low background γ detection, which can be achieved by the use of more sensitive detectors or more suitable shielding, can provide a remarkable increase in the signal/ background ratio. In this case the RDT signal will provide the direct measurement of the scattering signal, rather than a difference between two large count rates as in the SDT, so that higher statistical accuracy can be achieved.

A second result which has been assessed by the use of NaI detector is a neutron energy window up to 90 eV, including four distinct resonance peaks, as shown in Fig. 4.

This experiment has also allowed for the first time to demonstrate experimentally that a net decrease of the intrinsic width of the 6.6 eV resonance peak can be achieved by employing the double difference spectrum technique, with two uranium foils of different thickness, as suggested in previous papers [31].

In conclusion the present results provide a useful empirical basis for ongoing investigations of the Resonant Detector Technique using different combinations of resonant foils and γ detectors. We nevertheless believe that much better results should be expected by further improvements in the shielding design and, especially, by the use of more advanced γ detectors. It is therefore our intention to further investigate the use of different γ detectors, or combinations of detectors. In order to exploit the RDT in the neutron energy range 10-100 eV several improvements are envisaged. Most important is the signal/background ratio, which needs to be increased by over an order of magnitude. Since some background components scale with detector volume, it is mandatory to consider small detectors, which, however, can only detect low energy γ with adequate efficiency. A promising approach is to look for resonant foils that have a large probability (say, >50%) of emitting low energy γ's following resonant neutron capture. Several examples of suitable foils exist and will be tested in the near future. A second requirement concerns the time resolution of the measurements. As the neutron energy approaches 100 eV, the peaks in the time of flight spectrum become very narrow and an estimated time resolution of 50 ns appears to be required and can be met by scintillators and solid state detectors.

Another comment regards the count rate. Due to the large background, count rates exceeding 100 kHz were recorded with the present NaI detector. This was more than a regular spectroscopy amplifier could handle, so that time amplifiers had to be used instead. By going to low volume and low area detectors, the rate should be kept to suitable levels allowing full energy

analysis of the events. This is necessary in order to set tight γ energy windows for enhanced background rejection.

The ultimate solution in background suppression is the use of coincidence techniques. These have the drawback of decreasing the overall system efficiency by typically an order of magnitude. Depending on the intensity of the scattered neutron flux, coincidence techniques may turn out to be too costly in terms of beam-time requirements. They should nevertheless be investigated for applications where measurements of the highest quality are needed.

Acknowledgement

REFERENCES

[1] C. Andreani, A. Filabozzi, M. Nardone, F.P.Ricci and J. Mayers, Phys. Rev. B 50, 12744 (1994).

[2] J. Mayers and A. C. Evans, R.A.L. Report RAL-91-048, (1991).

[3] J Mayers, Phys. Rev. B41, 41 (1990).

[4] D. Colognesi, C. Andreani and R. Senesi, Europhys. Lett. 50, 202 (2000).

[5] D.N. Timms, A.C. Evans, M. Boninsegni, D.M. Ceperley, J. Mayers and R.O. Simmons, J. Phys. Cond. Matter 8, 6665-6684 (1996).

[6] G. Watson, J. Phys. Cond. Matter 8, 5955 (1996). E. Pace, G. Salmé, G. West, Phys. Lett. B, 273, 205 (1991).

[7] J. M. F. Gunn, C. Andreani and J. Mayers, J. Phys. C 19, 835 (1986).

[8] P. Postorino, F. Fillaux, J Mayers, J. Tomkinson and R S Holt J. Chem. Phys. 94, 4411 (1992); F. Fillaux, M.H. Baron, J. Mayers and J. Tomkinson, Chem. Phys. Lett. 240, 114 (1995).

[9] A. C. Evans, J. Mayers and D. N. Timms, Phys. Rev. B 53, 3023 (1996).

[10] A. L. Fielding, D. N. Timms, A.C. Evans and J. Mayers. J. Phys Cond. Matter 8, 7205-7219 (1996).

[11] P. C. H. Mitchell, D. A. Green, E. Payen and A. C. Evans J. Chem. Soc. Faraday Trans. 91, 4467-71 (1995)

[12] E. M. A. Gray, M. Kemali, J. Mayers and J. Noreland. J. Alloys and Compounds 253, 291-4 (1997).

[13] F.J. Bermejo,F.J. Mompean, J.Mayers and A C Evans. Phys. Lett. A189 333 (1994)

[14] J. Dawidowski, F.J. Bermejo, L. Fernandez Barquin, P. Gorria, J. M. Barandarian, A. C. Evans and J. Mayers. Phys. Lett. A 214, 59 (1996).

[15] J. Mayers, T.M. Burke and R. J. Newport J. Phys. Cond. Matter 6, 641 (1994).

[16] C. A. Dreismann, T. Abdul-Redah, R.M.F. Streffer and J. Mayers, Phys. Rev. Lett. 79, 2839 (1997).

[17] M. Celli, M. Zoppi, J. Mayers, Phys. Rev. B 58, 242 (1998).

[18] U. Bafile, M. Zoppi, F. Barocchi, R. Magli and J Mayers, Phys. Rev. Lett. 75, 1957 (1995); Phys. Rev. B 54, 11969 (1996).

[19] J. Mayers, C. Andreani and D. Colognesi. J. Phys. Cond. Matter 9, 10639-10649 (1997).

[20] A. R. Spowart, Nucl. Inst. Meth. 135, 441 (1976).

[21] R. J. Newport, J. Penfold, W. G. Williams, Nucl. Inst. Meth., 224, 120 (1984).

[22] A. D. Taylor, R. A. Robinson, P. A. Seeger, Nucl. Inst. Meth., 224, 133 (1984).

[23] D. R. Allen, E. W. Mitchell, R. N. Sinclair, J. Phys. E: Sci Instrum., 13, 639 (1980).

[24] R. M. Brugger, A. D. Taylor, C. E. Olsen, J. A. Goldstone, A. K. Soper, Nucl. Inst. Meth. 221, 393 (1984).

[25] N. Watanabe, International Atomic Energy Agency Proceedings, IAEA -- CN --46/26, 279 (1985)

[26] L. N. Cser, N. Kroo, P. Pacher, V. G. Simdon, E. V. Vasilieva, Nucl. Inst. Meth. 179, 515 (1981).

[27] R. G. Johnson, Nucl. Inst. Meth., A263, 427 (1988).

[28] J. M. Carpenter, N. Watanabe, S. Ikeda, Y. Masuda, S. Sato, Physica B 120, 126 (1983).

[29] H. Rauh, N. Watanabe, Nucl. Inst. Meth. 222, 507 (1984).

[30] G. F. Knoll, Radiation Detection and Measurement, John Wiley & Sons, New York (1999).

[31] P. A. Seeger, A. D. Taylor, R. M. Brugger, Nucl. Inst. Meth., A240, 98 (1985); C. Andreani, E. Degiorgi, A. Filabozzi, D. Colognesi, M. Nardone, 'Double Difference technique applied to Deep Inelastic Neutron Scattering on eVS spectrometer: U and Au foils'. Internal Report Rom2F/98/04, Dipartimento di Fisica Università di Roma Tor Vergata, 1998.

[32] S.F. Mughabghab, M. Divadeenam and N.E. Holden, Neutron cross-sections, Vol. 1 (Academic Press, New York, 1981).

[33] V. F. Sears, Phys. Rev. B 30, 45 (1984).

[34] G. B. West, Phys. Rep. 18, 263 (1975).

[35] C. Andreani, G. Baciocco, R. S. Holt, J. Mayers, Nucl. Inst. Meth. A276, 297 (1989).

[36] J. M. Blatt and V. F. Weisskopf, Theoretical Nuclear Physics (Springer New York 1952).